ROME 2008
LEVERAGING TECHNOLOGY

F029

Prestack Migration in Elliptic Coordinates

J.C. Shragge* (Stanford University) & G. Shan (Stanford University)

SUMMARY

Riemannian wavefield extrapolation is extended to prestack migration through the use of 2D elliptic coordinate systems. The corresponding 2D elliptic coordinate extrapolation wavenumber is demonstrated to introduce only a slowness model stretch to the single-square-root operator, enabling the use of existing Cartesian implicit finite-difference extrapolators to propagate wavefields. A post-stack migration example illustrates the advantages of elliptic coordinates in imaging overturning wavefields. Imaging tests of BP Velocity Benchmark data set illustrate that the RWE migration algorithm generates high-quality prestack migration images comparable to, or better than, the corresponding Cartesian coordinate systems.

Introduction

Wave-equation migration techniques based on one-way extrapolators are often used to accurately image structure in complex geologic environments. Most conventional downward continuation approaches, though, are unable to handle steeply propagating or overturning wavefield components often important for imaging areas of interest. A number of novel imaging approaches address these issues through a judicious decomposition of recorded wavefields (e.g. plane-wave migration (Etgen, 2002)), partial or complete propagation domain decomposition (e.g. Gaussian beam (Hill, 2001) or Riemannian wavefield extrapolation (Sava and Fomel, 2005), respectively), or a combination of these ideas (e.g. plane-wave migration in tilted coordinates (Shan and Biondi, 2004)). Importantly, these techniques have overcome many, though not all, issues in the practical application of one-way extrapolation operators.

Riemannian wavefield extrapolation (RWE) is a method for propagating wavefields on generalized coordinate meshes. The central idea behind RWE is to transform the geometry of the full domain to one where the extrapolation axis is oriented in the general wavefield propagation direction. Solving the corresponding one-way extrapolation equations propagates the bulk of wavefield energy at angles relatively close to the extrapolation axis, thus improving wavefield extrapolation accuracy. One obvious application is generating high-quality point-source Green's functions, where a ray-based coordinate system is generated by ray-tracing and used as the skeleton on which to propagate wavefields.

Although the full-domain decomposition approach naturally adapts to propagation in a point-source ray-coordinate system, two unresolved issues make it difficult to apply RWE efficiently in the prestack domain. First, receiver wavefields are usually broadband in plane-wave dip spectrum and cannot be easily represented by a single coordinate system (i.e. opposing dips propagate in opposing directions). Second, optimal source and receiver meshes usually do not share a common geometry. This factor is detrimental to algorithmic efficiency where generating images by correlating source and receiver wavefields: by existing on different grids they must both be interpolated to a common Cartesian reference frame prior to imaging. This leads to a significant number of interpolations that leaves the algorithm computationally unattractive.

The main goal of this paper is to specify a single coordinate system convenient for both the source and receiver wavefields that enables the accurate propagation of high-angle and turning wavefield components. To these ends, we demonstrate that an elliptic coordinate system is a 'natural' prestack migration coordinate system exhibiting nice geometric properties. An elliptic coordinate system originates on the surficial plane and expands outward as a series of ellipses. Thus, the coordinate system expands in a radial-like manner appropriate for computing accurate point-source Green's functions, while allowing the receiver wavefield to propagate at steep (and over-turning) angles to either side of the acquisition array where required. One consequence of using a 2D elliptic coordinate system is that the corresponding extrapolation wavenumber is specified by only a slowness model stretch. Thus, high-order implicit finite-difference extrapolators with accuracy up to 80º from the extrapolation axis (Lee and Suh, 1985) can be used to propagate wavefields, readily enabling accurate imaging of overturning waves at a cost competitive with downward continuation in Cartesian coordinates.

Why Elliptic Coordinates?

Generating a good coordinate system for RWE prestack migration requires appropriately linking mesh geometry with the dynamics of propagating wavefields. Figure 1 illustrates this for an idealized shot-profile imaging experiment that assumes source and receiver wavefields (S and R) are point sources defined at [$\mathbf{s}$, τ_s=0] and [$\mathbf{r}$, τ_r=0] in a constant velocity medium v($\mathbf{x}$). In this experimental setup, the wavefields expand outward as spherical wavefronts (dashed lines) described by

$$S(\mathbf{s},\mathbf{x},\mathbf{t}) = \delta\left(\mathbf{t} - \frac{||\mathbf{s}-\mathbf{x}||}{\mathbf{v}(\mathbf{x})}\right) \qquad \mathbf{R}(\mathbf{r},\mathbf{x},\mathbf{t}) = \delta\left(\mathbf{t} - \tau - \frac{||\mathbf{r}-\mathbf{x}||}{\mathbf{v}(\mathbf{x})}\right) \tag{1}$$

An image is generated by applying a correlation imaging condition at t =0,

$$I(\mathbf{x}) = \sum_{\mathbf{s}} \sum_{\mathbf{r}} \delta \left[\tau - \left(\frac{||\mathbf{x}-\mathbf{r}|| + ||\mathbf{x}-\mathbf{s}||}{\mathbf{v}(\mathbf{x})} \right) \right] \tag{2}$$

which is the equation of ellipse (solid line). This suggests a natural link between elliptic coordinate systems and prestack migration, which is evidenced in Figure 1 by the conformality of the drawn isochron and the coordinate mesh.

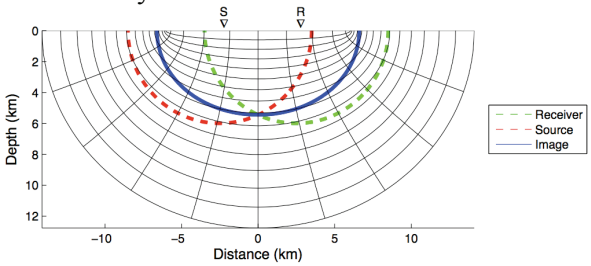

Figure 1. Idealized imaging experiment in a constant medium. Source and receiver wavefields (dashed lines) are expanding point sources described by S(**s**,**x**;t) and R(**r**,**x**;t). The corresponding image is the elliptic isochron surface I(**x**) (solid line).

The keen observer will note that in the foci of the elliptic coordinate system Figure 1 were not specified relative to **s** and **r**. Shifting these points around alters the mesh and how well it matches the isochrons. This represents two degrees of freedom that allow us to optimally match mesh geometry to the wavefield propagation dynamics.

Elliptic Coordinate Extrapolation

Propagating wavefields on elliptic meshes using RWE requires incorporating the geometry of the coordinate system directly in the extrapolation equations. This section derives the equations for propagation in the elliptic direction using the non-orthogonal RWE theory developed in Shragge (2006). The analytic transformation between the elliptic and Cartesian coordinate systems (see example in Figure 1) is specified by,

$$\begin{bmatrix} x_1 \\ x_3 \end{bmatrix} = \begin{bmatrix} a \cosh \xi_3 \cos \xi_1 \\ a \sinh \xi_3 \sin \xi_1 \end{bmatrix} \tag{3}$$

where [x_1,x_3] are the underlying Cartesian coordinate variables, [ξ_1,ξ_3] are the RWE elliptic coordinates, and a is a stretch parameter controlling the breadth of the coordinate system.

Metric tensor, g_{ij}, describing the geometry of the elliptic coordinate system is given by,

$$[g_{ij}] = \frac{\partial x_k}{\partial \xi_i} \frac{\partial x_k}{\partial \xi_j} = \begin{bmatrix} A^2 & 0 \\ 0 & A^2 \end{bmatrix} \tag{4}$$

where $A = a[\sinh^2\xi_3 + \sin^2\xi_1]^{1/2}$. The determinant of the metric tensor is $|\mathbf{g}|=A^4$, leading to an associated (inverse) metric tensor, g^{ij}, and weighted metric tensor (the product of the metric tensor and the determinant: m^{ij}) given by

$$[g^{ij}] = \begin{bmatrix} A^{-2} & 0 \\ 0 & A^{-2} \end{bmatrix} \qquad [m^{ij}] = \sqrt{|\mathbf{g}|} g^{ij} = \begin{bmatrix} 1 & 0 \\ 0 & 1 \end{bmatrix} \tag{5}$$

Note that even though the elliptic coordinate system varies spatially, the local curvature parameters in the weighted metric tensor are constant. We generate a wavenumber, $k_{\xi 3}$, for outward elliptic stepping recursive wavefield extrapolation by inserting tensors g^{ij} and m^{ij} into the wavenumber expression for a general 3D non-orthogonal coordinate systems (Shragge (2006), equations 13 and 14)

$$k_{\xi_3}^2 = \sqrt{\omega^2 s^2 A^2 - k_{\xi_1}^2} \tag{6}$$

where s is slowness and $k_{\xi 1}$ is the orthogonal wavenumber. Equation 6 is an exact extrapolation wavenumber that contains no kinematic approximation. The most striking observation about this expression is that the sole difference between propagation in elliptic and Cartesian coordinate systems is a smooth multiplicative slowness model stretch. Otherwise, existing Cartesian extrapolators can be used for propagating wavefields.

2D Synthetic Tests

This section presents 2D test results for a poststack overturning wavefield and the prestack Pluto data sets. We propagate all wavefields with the isotropic one-way extrapolator described in Lee and Suh (1985) on an elliptic coordinate system defined by equation 3 assuming effective slowness fields of s_{eff}=As where the stretch factor A is defined above. Generic post-stack and shot profile algorithms employing the extrapolation wavenumber in equation 6 are used for the following migrations. Elliptic coordinate migration results are interpolated back to Cartesian using sinc-based functions.

The first elliptic coordinate migration example uses the post-stack dataset shown in the upper panel of Figure 2. The data, generated by Sava (2006) from an adapted SMAART JV Pluto 1.5 model using exploding reflector modeling from all salt body edges, were recorded at all surface locations.

Figure 3 shows the migrated image obtained by elliptic coordinate RWE. The upper left panel shows the prestack migration result for a monochromatic wavefield. As expected for exploding reflector modeling, the monochromatic wavefield turns and arrives at the dipping salt flank at normal incidence. Note also that the wavefield energy propagates at a fairly steep angle to the extrapolation axis indicating that high-angle accuracy extrapolators are necessary for accurate imaging. The upper right panel shows the same image as the upper left, but in the elliptic coordinate system. The lower left and right panels show the broadband image results in Cartesian and elliptic coordinate systems, respectively. The salt flanks beneath the salt nose are accurately positioned, indicating a potential for imaging turning waves in elliptic coordinates with high-angle propagators.

Figure 4 presents a 2D prestack RWE migration result for the BP velocity benchmark model. The upper and lower panels show the elliptic and Cartesian RWE images, respectively. The upper panel image shows improvements (circled) in reflector amplitudes of the root of the right salt body. Note also that the steep flank on the left salt body is more continuous, unlike the corresponding reflector in the Cartesian image.

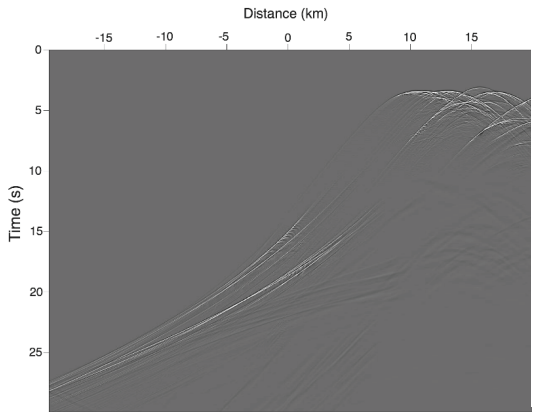

Figure 2. Data used in post-stack migration imaging experiment (Sava, 2006).

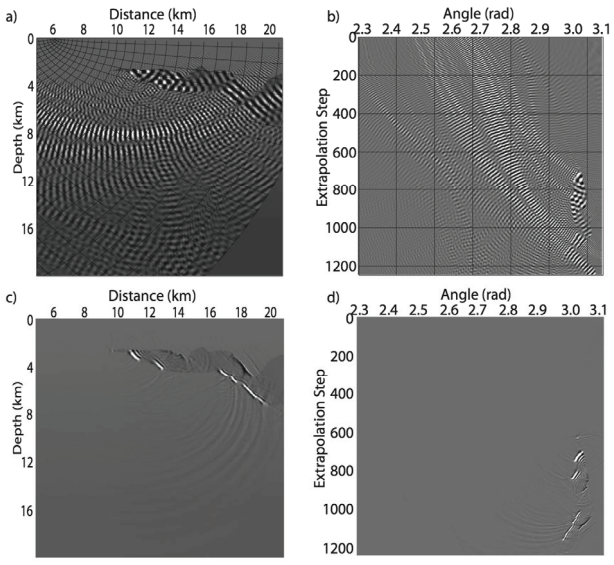

Figure 3. Post-stack elliptic migration example. a) Elliptic monochromatic wavefield in Cartesian coordinates. b) As in a) but in elliptic coordinates. c) Broadband version of a). d) Broadband version of b).

One question naturally arising when using RWE for propagation in prestack migration is how does one obtain the optimal trade-off between: i) incorporating wave-propagation effects directly in a more dynamic coordinate system (e.g. through a ray-traced coordinate system); and ii) using higher-order extrapolators in coordinate systems not strictly conformal to the

wavefield propagation direction. Based on our experience, we argue that a parametric coordinate system (such as tilted Cartesian or elliptic meshes) offers the advantage of being able to develop analytic extrapolation operators that readily lend themselves to accurate, high-order, finite-difference schemes. Though coordinate systems based on ray-tracing better conform to the direction of wavefield extrapolation, numerically generated meshes do not lend themselves as easily to high-order extrapolators due to a greater number of more spatially variable mixed-domain coefficients.

Concluding Remarks

This paper extends the theory of Riemannian wavefield extrapolation to prestack migration. An elliptic coordinate system is chosen because it generally conforms to the direction of propagation and allows high-angle propagation of source and receiver wavefields. Post-stack migration results of an overturning wavefield data set validate the approach, while the 2D prestack imaging results show that the RWE migration algorithm generates high-quality migration images comparable to, or better than, the corresponding Cartesian domain.

Acknowledgements

We thank Biondo Biondi, Ben Witten and Brad Artman for enlightening discussions. We thank the SEP sponsors for support and BP for the Velocity Benchmark data set.

References

Etgen, J., 2002, Waves, beams and dimensions: An illuminating if incoherent view of the future of migration: SEG

Hill, N. R., 2001, Prestack Gaussian-beam depth migration: Geophysics, 66, 1240–1250.

Lee, M. W., and S. Y. Suh, 1985, Optimization of one-way wave-equations: Geophysics, 50, 1634–1637.

Sava, P., 2006, Imaging overturning reflections by Riemannian wavefield extrapolation: Journal of Seismic Exploration, 15, 209–223.

Sava, P. C., and S. Fomel, 2005, Riemannian wavefield extrapolation: Geophysics, 70, no. 3, T45–T56.

Shan, G., and B. Biondi, 2004, Imaging overturned waves by plane-wave migration in tilted coordinates: 74th Annual International Meeting, SEG, Expanded Abstracts, 969–972.

Shragge, J., 2006, Non-orthogonal Riemannian wavefield extrapolation: 76th Annual International Meeting, SEG, Expanded Abstracts, 2236–2240.

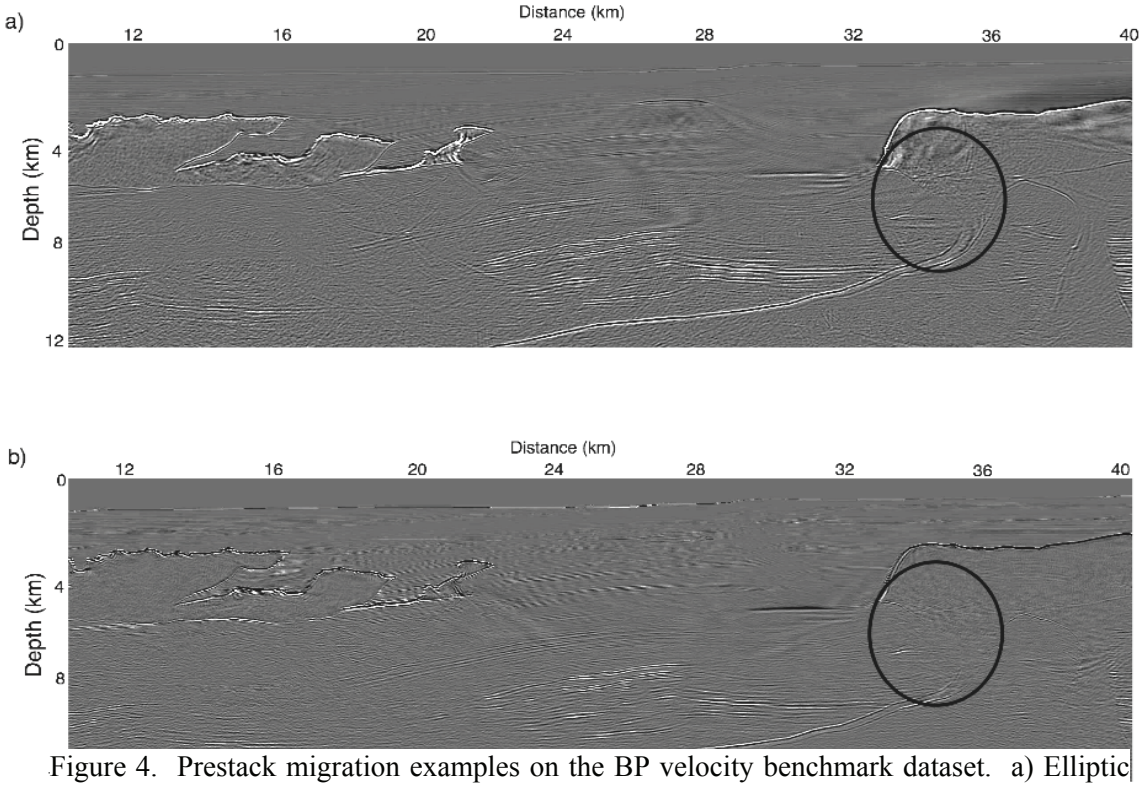

Figure 4. Prestack migration examples on the BP velocity benchmark dataset. a) Elliptic coordinate migration. b) Cartesian coordinate migration.